

## Oxidation-Process Dependence of Single Photon Sources Embedded in 4H-SiC MOSFETs

Yuta Abe<sup>1,a</sup>, Takahide Umeda<sup>1,b\*</sup>, Mitsuo Okamoto<sup>2,c</sup>, Shinobu Onoda<sup>3,d</sup>,  
Moriyoshi Haruyama<sup>3,4,e</sup>, Wataru Kada<sup>4</sup>, Osamu Hanaizumi<sup>4</sup>, Ryoji Kosugi<sup>2,f</sup>,  
Shinsuke Harada<sup>2,g</sup>, and Takeshi Ohshima<sup>3,h</sup>

<sup>1</sup>Institute of Applied Physics, University of Tsukuba, Tsukuba, 305-8573, Japan

<sup>2</sup>National Institute of Advance Industrial Science and Technology, Tsukuba, 305-8568, Japan

<sup>3</sup>National Institutes for Quantum and Radiological Science and Technology, 1233 Watanuki,  
Takasaki, Gunma, 370-1292, Japan

<sup>4</sup>Gunma University, 1-5-1 Tenjincho, Gunma, 376-0052, Japan

<sup>a</sup>s1620318@u.tsukuba.ac.jp, <sup>b</sup>umeda@bk.tsukuba.ac.jp, <sup>c</sup>mitsuo-okamoto@aist.go.jp,  
<sup>d</sup>onoda.shinobu@qst.go.jp, <sup>e</sup>haruyama.moriyoshi@qst.go.jp, <sup>f</sup>r-kosugi@aist.go.jp,  
<sup>g</sup>s-harada@aist.go.jp, <sup>h</sup>ohshima.takeshi@qst.go.jp

**Keywords:** single photon source, MOSFET, MOS interface, confocal microscope

**Abstract.** We investigated single photon sources (SPSs) in 4H-SiC metal-oxide-semiconductor field-effect transistors (MOSFETs) by means of confocal microscope techniques. We found SPSs *only* in 4H-SiC/SiO<sub>2</sub> interface regions of wet-oxide C-face MOSFETs. The other regions of MOSFETs such as source, drain and well did not exhibit SPSs. The luminescent intensity of the SPSs at room temperature was at least twice larger than that of the most famous SPSs, the nitrogen-vacancy center, in diamond. We examined four types of C-face and Si-face 4H-SiC MOSFETs with different oxidation processes, and found that the formation of the SPSs strongly depended on the preparation of SiC/SiO<sub>2</sub> interfaces.

### Introduction

Wide-bandgap semiconductors, especially diamond, have good color centers that are suitable for single photon sources (SPSs) operable at room temperature. Such “room-temperature SPSs” have a great potential for quantum photonics and quantum sensing applications. For example, if they have electron spins, they are usable as a quantum sensor for electromagnetic fields and are applicable to, e.g., bio-imaging technologies. The nitrogen-vacancy (NV) center in diamond realizes such an imaging [1]. However, diamond is known to be a high-cost material as well as having many difficulties for device processing.

On the other hand, it has been recently demonstrated that silicon carbide (SiC) is also a good host material for preparing room-temperature SPSs. For instance, a silicon-vacancy center ( $V_{Si}$ ) created by electron irradiation was demonstrated as room-temperature SPSs with electron spins [2]. Carbon antisite-vacancy pair ( $C_{Si}V_C$ ) in irradiated high-purity semi-insulating 4H-SiC was also found to act as bright SPSs [3]. Room-temperature SPSs were also simply formed by a low-temperature oxidation of SiC surfaces [4]. Furthermore, room-temperature SPSs (tentatively assigned to an antisite center) were found in 4H-SiC *pn* diodes, which were electrically driven by pulse currents [5]. Recently, we have found room-temperature SPSs in the channel regions (SiC/SiO<sub>2</sub> interfaces) of 4H-SiC MOSFETs [6]. Their signatures were significantly different from the SPSs reported in previous works [2-5], and hence we assigned them to a novel type of SPSs [6]. These SPSs have a possibility to control their charge states and spin states by an electrical voltage or current of a MOSFET. We believe that they were formed at the 4H-SiC/SiO<sub>2</sub> interfaces; namely, they are a sort of interface defects. Therefore, in this work, we examined oxidation-process dependences of the interfacial SPSs by preparing four types of 4H-SiC MOSFETs with different oxidation processes.

## Experiments

We used a home-built confocal microscope (CFM) using high-NA ( $NA = 0.95$ ) air object lens and a 532-nm laser to detect photoluminescence (PL) from a single PL center. This is optimized for observing the  $NV^-$  center in diamond [7]. A confocal beam is detected by a pair of avalanche photo diodes. In this work, we measured  $X$ - $Y$ - $Z$  mapping images (positional resolution  $\geq 1$  nm) as well as performed anti-bunching measurements with a Hanbury-Brown-Twiss interferometer [2-5]. The laser light and PL emissions below 647 nm are cut off by a long-pass filter to highlight spots of SPSs. Using our CFM setup, a single  $NV^-$  center can be detected as a bright spot with a diameter of  $0.5 \mu\text{m}$  and a peak luminescent intensity of 80,000 counts-per-sec (80 kcps).

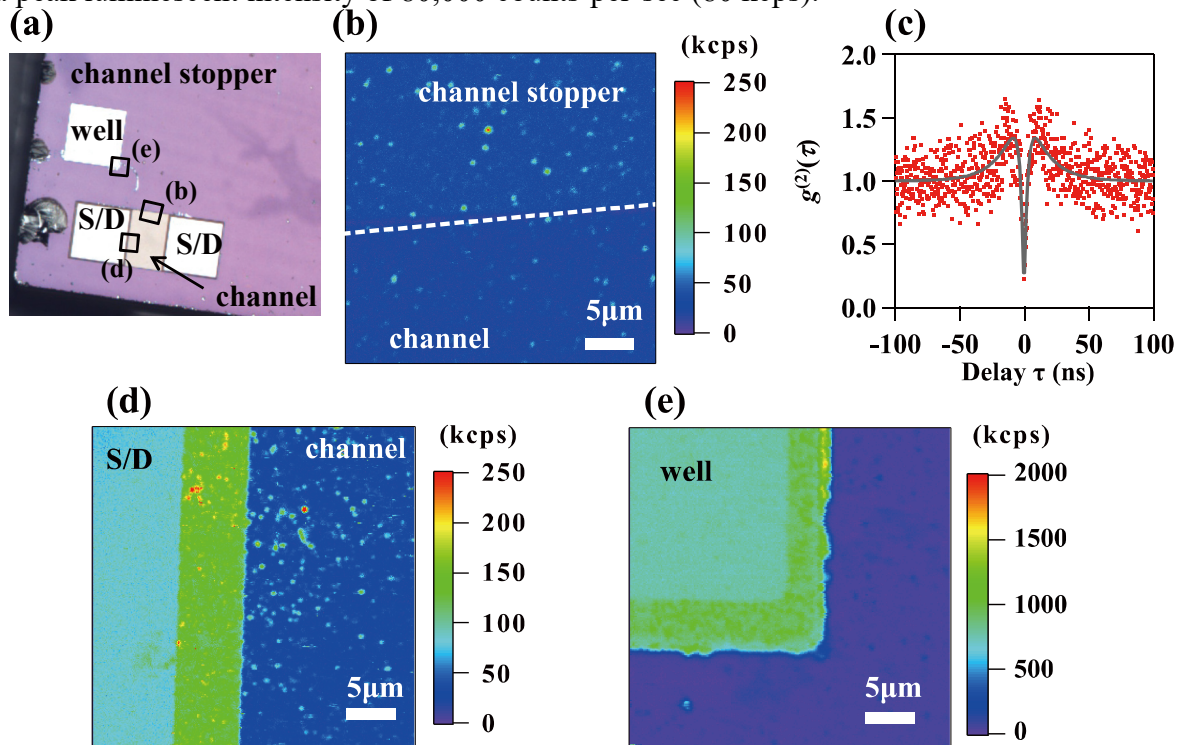


Fig. 1. (a) Optical microscope image of an wet-oxide C-face 4H-SiC MOSFET after removing Al electrodes. (b) An  $X$ - $Y$  CFM image of the channel and channel-stopper regions. The bright spots of  $\sim 160$  kcps arise from SPSs. (c) Anti-bunching behavior of a SPS in the channel region. (d) An  $X$ - $Y$  CFM image of the S/D and the channel regions. The S/D region exhibits no SPSs, while many bright spots of the SPSs exist in the channel region. (e) An  $X$ - $Y$  CFM image of the well region. The well region also did not show SPSs (the SPSs in the channel-stopper region are also not visible because of a wider color-scale range). The CFM images (b), (d) and (e) were obtained from the rectangular regions shown in (a).

The samples we measured are four types of  $n$ -channel lateral C-face and Si-face 4H-SiC MOSFETs (gate oxide thickness = 50 nm, gate length/width = 100/150  $\mu\text{m}$ ). The C-face samples were prepared by either wet oxidation at 1000  $^{\circ}\text{C}$  or dry oxidation at 1100  $^{\circ}\text{C}$  on a 5- $\mu\text{m}$  epitaxial layer of a  $4^{\circ}$ -off 4H-SiC(000 $\bar{1}$ ) wafer. On the other hand, the Si-face ones were subjected to either the standard dry oxidation or the standard post-oxidation nitridation (NO anneal). Figure 1 (a) shows the whole image of a MOSFET used for CFM measurements. There are four types of doped regions, “ $n^+$ -type source and drain (S/D),” “ $p^+$ -type well,” “ $p^-$ -type channel,” and “ $p^-$ -type channel stopper.” In order to examine these regions by CFM, metal electrodes were removed by a wet etching, as the  $\text{SiO}_2$  layers remained as they were. The channel region was covered by a 50-nm-thick thermal oxide, while the channel-stopper region was covered by a 500-nm-thick deposited  $\text{SiO}_2$  layer. In CFM measurements, we focused on SiC surfaces of the S/D and well regions or SiC/ $\text{SiO}_2$  interfaces of the channel and channel-stopper regions. All CFM measurements were carried out at room temperature and under 1-mW laser excitation.

## Results

Figure 1(b) shows a CFM image of the boundary between the channel and channel-stopper regions of a wet-oxide C-face MOSFET. Both regions show many isolated bright spots, which are arising from SPSs. The peak luminescent intensities of the spots are about 160 kcps, which are twice larger than that of the  $NV^-$  center (80 kcps). To confirm that the observed spots are surely SPSs, we carried out the anti-bunching measurements [2-5]. Figure 1(c) shows the normalized self-correlation function  $g^{(2)}(\tau)$  measured for a bright spot in the channel region, where  $\tau$  is a delay time between photon-detection events of the two independent photo detectors. The anti-bunching curve can be well fitted by the case of a SPS with a three-level PL system [8], demonstrating the presence of a SPS in a single spot. Also the bright spots in the channel-stopper region revealed similar  $g^{(2)}(\tau)$  curves as well as the same luminescent intensities as those of the SPSs in the channel region. Therefore, we judged that the SPSs in the channel and channel-stopper regions are identical.

On the other hand, the S/D region and the well region were overall very bright and exhibited no SPSs [Figs. 1(d) and (e), respectively]. Instead, these regions showed high background luminescence of  $\sim 100$  kcps (S/D) and  $\sim 750$  kcps (well), which were much brighter than that of the channel and channel-stopper regions ( $\sim 25$  kcps). Since the S/D and well regions were subjected to high-dose ion implantations, dopants and implantation damages may cause the bright background luminescence.

To investigate the oxidation-process dependence of the SPSs, we measured other three types of MOSFETs. Figures 2(a) to (d) compare CFM images of the channel regions (upper half) and the channel-stopper regions (lower half) of the MOSFETs with different gate-oxide processes. Only in (a) (C-face wet oxidation), were the bright spots of the SPSs observed. The areal density of the SPSs was estimated to be  $1 \times 10^7 \text{ cm}^{-2}$  in both regions (see Table I). In Fig. 2(b) (C-face dry oxidation), both regions emitted overall bright background. However, the luminescent spots could be slightly recognized. Their areal densities were more than 20 times higher than those of (a) (see Table I), and we could not observe anti-bunching behaviors in any those spots. Even with the high density of the spots, the dry-oxide C-face interface exhibited a lower luminescent intensity (see Table I). Therefore, we suggest different origins for the luminescent spots in (a) and (b). The channel and channel-stopper regions of the two Si-face SiC-MOSFETs [Figs. 2(c) and (d)] revealed spotty images more similar to Fig. 2(a). The areal densities of the luminescent spots were about  $1 \times 10^8 \text{ cm}^{-2}$  (see Table 1), which we expect will enable us to observe individual SPSs. However, we could not find any anti-bunching behaviors in the two Si-face SiC-MOSFETs. This result is contrast with the previous work that observed SPSs in a briefly oxidized 4H/6H/3C-SiC surfaces [3]. The CFM observations of the four MOSFETs are summarized in Table 1, which clearly indicates that the formation of the SPSs depends on oxidation processes.

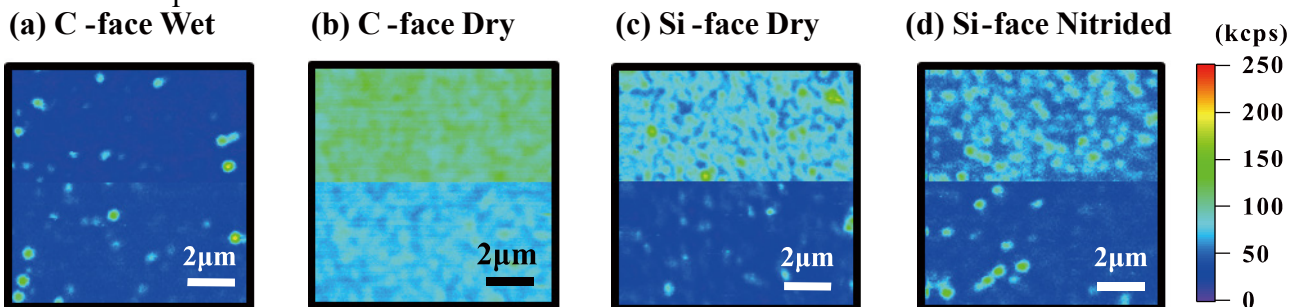


Fig. 2. Comparison of X-Y CFM images in the channel (upper half) and the channel-stopper (lower half) regions of four types of 4H-SiC MOSFETs with (a) C-face wet-oxide, (b) C-face dry-oxide, (c) Si-face dry-oxide, and (d) Si-face dry-oxide + standard NO nitridation.

Table I. Properties of the luminescent spots in four types of SiC-MOSFETs.

	C-face				Si-face			
	Wet oxidation		Dry oxidation		Dry oxidation		Nitrated	
	ch <sup>*1</sup>	ch-st <sup>*1</sup>	ch	ch-st	ch	ch-st	ch	ch-st
Areal density [ $\times 10^8 \text{ cm}^{-2}$ ]	0.1	0.1	2.9	2.3	1.2	1.0	0.7-1.0	0.3
Spot [kcps]	> 160	> 160	100-120	100-120	100	80	120-130	> 160
Background [kcps]	20-30	20-30	80-90	60	50-60	20-30	50-60	30-40
Anti-bunching behavior	○	○	×	×	×	×	×	×

\*1 “ch” and “ch-st” mean the channel region and the channel-stopper region, respectively.

## Summary

We have found the SPSs in the channel and the channel-stopper regions of wet-oxide C-face 4H-SiC MOSFETs. They were brighter than the  $NV^-$  center in diamond within our CFM setup. In the same MOSFET, the S/D region and the well region revealed no SPSs, and exhibited very high background luminescence. We also examined dry-oxide C-face MOSFETs as well as two types of Si-face MOSFETs. The dry-oxide C-face sample did not show the SPSs, indicating a strong dependence of the SPSs on oxidation processes. Also in the Si-face MOSFETs, we did not find any SPSs, which is contrast with the previous works (e.g., Ref. 3) that reported a simple formation of SPSs via a brief oxidation of Si-face SiC surfaces.

## Acknowledgements

This work was partly supported by the JSPS KAKENHI Grant Nos. 26286047 and 17H01056.

## References

- [1] Hui, Y. Y., Cheng, C-L. & Chang, H-C, *J. Phys. D* **43**, 374021 (2010).
- [2] M. Widmann, S.-Y. Lee, T. Rendler, N. Tien Son, H. Fedder, S. Pirk, L.-P. Yang, N. Zhao, S. Yang, I. Booker, A. Denisenko, M. Jamali, S.A. Momenzardeh, I. Gerhardt, T. Ohshima, A. Gali, E. Janzén, J. Warchtrup, *Nat. Mater.* **14**, 164 (2015).
- [3] S. Castelletto, B. C. Johnson, V. Ivády, N. Stavrias, T. Umeda, A. Gali, T. Ohshima, *Nat. Mater.* **13**, 151 (2014).
- [4] A. Lohrmann, S. Castelletto, J. R. Klein, T. Ohshima, M. Bosi, M. Negri, D. W. M. Lau, B. C. Gibson, S. Praver, J. C. McCallum, B. C. Johnson, *Appl. Phys. Lett.* **108**, 021107 (2016).
- [5] A. Lohrmann, N. Iwamoto, Z. Bodrog, S. Castelletto, T. Ohshima, T. Karle, A. Gali, S. Praver, J. McCallum, B. C. Johnson, *Nat. Commun.* **6**, 7783 (2015).
- [6] Y. Abe, T. Umeda, M. Okamoto, R. Kosugi, S. Harada, M. Haruyama, W. Kada, O. Hanaizumi, S. Onoda, T. Ohshima, *Appl. Phys. Lett.* **112**, 031105(2018).
- [7] S. Onoda, M. Haruyama, T. Teraji, J. Isoya, W. Kada, O. Hanaizumi, T. Ohshima, *phys. stat. sol. (a)* **212**, 2641 (2015).
- [8] B. Lienhard, T. Schröder, S. Mouradian, F. Dolde, T. T. Tran, I. Aharonovich, D. Englund, *Optica* **3**, 768-774 (2016).